Poloxamer 188 Decreases Susceptibility of Artificial Lipid Membranes to Electroporation

Vinod Sharma,* Kathleen Stebe,# John C. Murphy,§ and Leslie Tung*
*Department of Biomedical Engineering, The Johns Hopkins University, Baltimore, Maryland 21205 USA, #Department of Chemical Engineering, The Johns Hopkins University, Baltimore, Maryland 21218 USA, and §Sensor Science Group, Applied Physics Lab, The Johns Hopkins University, Laurel, Maryland 20723 USA

ABSTRACT The effect of a nontoxic, nonionic block co-polymeric surface active agent, poloxamer 188, on electroporation of artificial lipid membranes made of azolectin, was investigated. Two different experimental protocols were used in our study: charge pulse and voltage clamp. For the charge pulse protocol, membranes were pulsed with a 10-μs rectangular voltage waveform, after which membrane voltage decay was observed through an external 1-MΩ resistance. For the voltage clamp protocol the membranes were pulsed with a waveform that consisted of an initial 10-μs rectangular phase, followed by a negative sloped ramp that decayed to zero in the subsequent 500 μs. Several parameters characterizing the electroporation process were measured and compared for the control membranes and membranes treated with 1.0 mM poloxamer 188. For both the charge pulse and voltage clamp experiments, the threshold voltage (amplitude of initial rectangular phase) and latency time (time elapsed between the end of rectangular phase and the onset of membrane electroporation) were measured. Membrane conductance (measured 200 μs after the initial rectangular phase) and rise time (t_r; the time required for the porated membrane to reach a certain conductance value) were also determined for the voltage clamp experiments, and postelectroporation time constant (PEτ; the time constant for transmembrane voltage decay after onset of electroporation) for the charge pulse experiments. The charge pulse experiments were performed on 23 membranes with 10 control and 13 poloxamer-treated membranes, and voltage pulse experiments on 49 membranes with 26 control and 23 poloxamer-treated membranes. For both charge pulse and voltage clamp experiments, poloxamer 188-treated membranes exhibited a statistically higher threshold voltage ($p = 0.1$ and $p = 0.06$, respectively), and longer latency time ($p = 0.04$ and $p = 0.05$, respectively). Also, poloxamer 188-treated membranes were found to have a relatively lower conductance ($p = 0.001$), longer time required for the porated membrane to reach a certain conductance value ($p = 0.05$), and longer postelectroporation time constant ($p = 0.005$). Furthermore, addition of poloxamer 188 was found to reduce the membrane capacitance by ~4-8% in 5 min. These findings suggest that poloxamer 188 adsorbs into the lipid bilayers, thereby decreasing their susceptibility to electroporation.

INTRODUCTION

Electrical fields, pulsed as well as continuous, are used for a variety of cellular manipulations (Neumann et al., 1989). Among them are cell rotation, pearl chain formation, cell fusion, and electroporation. Sale and Hamilton (1967) were the first to observe that the application of an electric field in the range of a few kV/cm led to cell lysis or death. They attributed this to the dielectric breakdown of membrane and loss of its barrier properties in response to the high transmembrane voltage (~1 V) induced by the applied electric field. This phenomenon was later found to be fundamentally different from other experiments in which Neumann and Rosenheck (1972) showed that application of electric fields of sufficient strength, but below a critical intensity, can cause biomembranes to enter a transient high permeability state. In this high permeability state the membrane can allow passage of ions and macromolecules. Artificial lipid membranes that serve as useful models for cell membranes also exhibit an increase in permeability on exposure to transmembrane voltage above a threshold value (Abidor et al., 1979; Chernomordik et al., 1983; Sharma et al., 1994b). The phenomenon has been commonly termed as electroporation (for a review see Tsong, 1991 and Weaver, 1995).

One mechanism underlying electroporation comes from the research groups of Chizmadzhev (Chizmadzhev et al., 1979) and Weaver (in Freeman et al., 1994). These investigators postulate that electroporation is a stochastic process and that the high transmembrane voltage reduces the energy barrier for the thermally driven formation of hydrophilic pores from the preexisting hydrophobic pores in the membrane. Another mechanism based on a mechanical stability framework was originally posed by Crowley (1971). According to this mechanism, the membrane porates at a critical field strength dependent on membrane physical properties. For an isotropic membrane the critical voltage and electrocompression were predicted to be in excess of those observed experimentally. These discrepancies can be resolved by assuming the membrane to be anisotropic in its elastic response to deformation and shear (Maldarelli and Stebe, 1992).

Electroporation is widely used for gene transfection (Kubiniec et al., 1990; Wolf et al., 1994) and for introducing membrane impermeant macromolecules into cells (Chalm

Received for publication 1 April 1996 and in final form 5 September 1996.
Address reprint requests to Dr. Leslie Tung, Department of Biomedical Engineering, the Johns Hopkins University, 720 Rutland Avenue, Baltimore, MD 21205. Tel.: 410-955-7453; Fax: 410-955-0549; E-mail: ltung@bme.jhu.edu.

0006-3495/96/12/3229/13 $2.00

ers, 1985; Sixou and Teissie, 1993). Also, electroporation holds promise to be used for transdermal drug delivery (Prausnitz et al., 1993; Vanbever et al., 1994) and for enhancing the effects of anti-cancer drugs specifically at the site of subcutaneous tumors (Okino and Mohri, 1987; Mir et al., 1991; Belehradek et al., 1993).

In contrast to these important applications in which electroporation is desired, it is postulated that electroporation may be one of the main injury mechanisms to skeletal and nerve cells during unintentional application of strong electrical shock as in an electrical trauma (Gaylor et al., 1992), and to cardiac cells in situations where strong electrical shock may be applied to the heart, such as during internal defibrillation or ablation (Tung, 1992; Tung et al., 1994). It is believed that if electropores persist for long times compared to the time required for the diffusion of ions and cellular metabolites through the pores, chemical and osmotic imbalances can develop in the cells. In the extreme case these imbalances can result in cell death and tissue necrosis. For all cell types, electropore-mediated rise of intracellular Ca^{2+} is believed to be one of the main causes of cellular dysfunction and death. Elevated levels of intracellular Ca^{2+} can induce cell injury by a multitude of pathways, including abnormal activation or inhibition of key enzymes, organelle disruption, denaturation of essential cellular proteins, and depletion of ATP (Trump and Berezesky, 1995). The electropore-mediated influx of Ca^{2+} can cause hyperactivation of calpain, a Ca^{2+}-sensitive protease, which can degrade cytoskeletal filaments like spectrin (Hong et al., 1994) and result in altered cytoskeletal dynamics. Loss of essential cellular enzymes and metabolites through larger diameter pores are also likely to play a role in cell injury (for discussions addressing membrane pore-mediated injury to skeletal and cardiac cells refer to Gaylor et al., 1992, and Tung, 1992, respectively).

Therefore, it appears that to alleviate the tissue injury caused by intentional or unintentional application of high electric fields, techniques to repair the membrane holes, or modify the membranes to decrease their susceptibility to electroporation for a given applied electric field, need to be developed. Recently, there have been studies on biological (Lee et al., 1992) and artificial membranes (Sharma et al., 1994a; Sharma and Tung, 1995), which explore the possibility of using the compound poloxamer 188 to treat the membranes to achieve these goals.

Poloxamer 188 or Pluronic F-68 (MW: ~8400) belongs to a family of more than 30 different nontoxic (Schmolka, 1972; Johnston and Miller, 1985) nonionic surface active agents and was one of the first poloxamers commercially available that has found a myriad of clinical applications (for a review see Schmolka, 1994). Among its most important applications are its use as a skin wound cleanser (Rodeheaver et al., 1980), an emulsifying agent in artificial blood (Schmolka, 1975; Mitsuno, 1984), an anticoagulant of the microcirculation (Hymes et al., 1970), and an agent to reduce reperfusion-induced injury to the myocardium (Kolodgie et al., 1994). Recently, Padanilam et al. (1994) have shown the effectiveness of poloxamer 188 in arresting the leakage of the fluorescent dye calcein from skeletal muscle cells that were exposed to supraphysiological temperatures ranging from 37°C to 60°C. Thus, poloxamer 188 also holds promise for reducing thermally induced injury.

In vitro and in vivo studies by Lee et al. (1992) on isolated skeletal muscle cells and rat muscle flap, respectively, suggested that postelectroporation administration of poloxamer 188 seals electropores and substantially reduces tissue injury. Another finding of their study was that the intravenous pretreatment of muscle flap with poloxamer 188 was effective in restoring the flap impedance (a measure of cell membrane impedance) close to its preelectroporation baseline value in a *dose-dependent* manner. This prompted us to hypothesize that poloxamer 188 is able to interact with a cell membrane and render it more resistant to electroporation. Indeed, it has been established that poloxamer 188 adsorbs into a lipid monolayer (analogous to a single leaflet of a cell membrane without its proteins) spread at a water-air interface (Magalhaes et al., 1991; Weingarten et al., 1991). Electropores are believed to form mainly in the lipid matrix of a cell membrane, although membrane proteins might play a role in their stability and time of resealing (Weaver and Barnett, 1992). Hence, the ability of poloxamer 188 to reduce electroporation-mediated tissue injury is likely to occur via its interaction with the lipid matrix of the membrane. For this reason we studied the effect in artificial lipid bilayers of pretreatment with poloxamer 188 on the threshold voltage and kinetics of electroporation.

The two common methods for studying electroporation in lipid bilayers are charge pulse (Benz et al., 1979; Klotz et al., 1993; Wilhelm et al., 1993) and voltage clamp (Abidor et al., 1979; Chernomordik et al., 1983; Sharma et al., 1994). Membrane electroporation can be characterized using several parameters, including threshold voltage, latency time, or membrane lifetime (Abidor et al., 1979; Wilhelm et al., 1993), membrane conductance, and postelectroporation time constant (PEτ), a new parameter introduced in this paper. The exact definitions of these parameters are given in the Materials and Methods and Results sections of this paper. Therefore, the effect of poloxamer on membranes can be studied by identifying differences in these parameters for control and poloxamer-treated membranes. We initiated our study by using the charge pulse method because it utilizes simpler circuitry compared with the voltage clamp method. However, because of its advantage in allowing membrane conductance to be monitored over longer durations, we also used the voltage clamp method. The circuitry used for our charge pulse experiments was similar to that of Benz et al. (1979) except that we connected an external 1-MΩ resistance (R_e) in parallel with the membrane. The purpose of this resistance was to enable measurement of membrane capacitance (C_m) by estimating the time constant (τ) of membrane discharge. Our findings regarding the effect of poloxamer 188 on membrane electroporation using these two common protocols is reported in this paper.

MATERIALS AND METHODS

Bilipid membranes were formed from a solution of 20 mg azolectin, (Avanti Polar Lipids, Alabaster, AL) dissolved in 1 ml pentane (Fluka Chemical, Ronkonkoma, NY) across a 75–100-μm diameter hole in a 25-μm thick Teflon sheet (Chemfab, Merrimack, NH) mounted in a custom-designed bilayer chamber (Fig. 1), using the folding method (White, 1986). These holes were made either by using a high-power laser or by applying a high-voltage RF pulse across the Teflon sheet.

Before the Teflon sheet was mounted in the chamber, it was first washed in a continuous stream of deionized water and then soaked in ethanol. After ~5 min the Teflon sheet was removed from the ethanol, allowed to dry, and washed in chloroform. This procedure removed all the hydrophobic and hydrophilic impurities from the Teflon sheet. The hole was then treated with ~0.5 μl of a solution containing 10% hexadecane in pentane and was allowed to dry for ~5 min. This procedure left a small amount of hexadecane at the hole, which formed the torus by which the membranes were supported at their edges (White, 1972).

The folding method for forming a lipid membrane was as follows. After mounting the Teflon sheet in the bilayer chamber, both compartments of the chamber were filled with KCl (100 mM, pH 7.23) and the solution level was adjusted to be just below the hole. A drop (~10 μl) of lipid solution was carefully deposited on the aqueous-air interface on each side of the Teflon sheet, and was allowed to spread to form a monolayer on the interface. The solution level in both compartments of the chamber was then gradually raised. As the two monolayers were raised past the hexadecane-coated hole, their hydrocarbon chains apposed each other to form a bilayer. After a membrane was exposed to an electroporating pulse, it underwent irreversible rupture. A new membrane was formed by bringing the solution level below the hole and again raising it above the hole.

The experimental system (Fig. 1) used a specially designed high-speed, low-charge injection analog switch (S). The switch was built by combining an analog switch (LF11333; National Semiconductor Corp., Santa Clara, CA) with positive-charge injection in parallel with another analog switch (IH5048; Maxim Integrated Products, Sunnyvale, CA) with equal but negative charge injection. The switch had a very low "on" resistance, which allowed rapid (<10 ns) charging of the membrane and a very high "off" resistance, which isolated the membrane from the voltage source, and allowed the membrane discharge to be observed through an external 1-MΩ resistance. Low-charge injection (Q_{inj}) of the switch was desirable to ensure a minimal artifactual jump in transmembrane voltage, given by

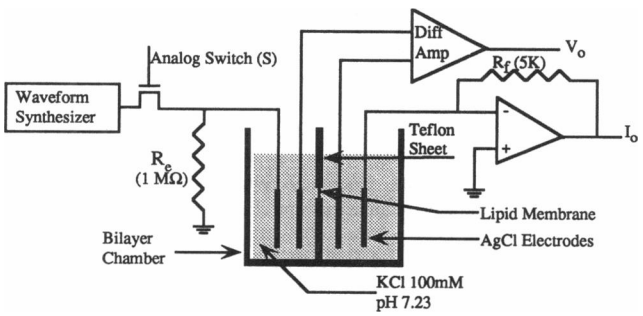

FIGURE 1 Schematic of the experimental setup. A Teflon sheet with a hole ~100 μm in diameter was sandwiched between two KCl-filled compartments of a bilayer chamber and a lipid bilayer was formed across the hole using the folding method (see text). The setup employed four fast Ag-AgCl electrodes; two central electrodes were used to measure transmembrane voltage (V_o) via a high-impedance differential amplifier, and the remaining two peripheral electrodes were used to apply voltage pulses across the membrane and measure transmembrane current (I_o). Analog switch (S) isolated the membrane from voltage source after application of an electroporating pulse and allowed membrane voltage to decay only through an external 1-MΩ resistance (R_e). Voltage source consisted of an arbitrary waveform synthesizer board interfaced to an IBM-PC clone.

Q_{inj}/C_n (where C_n was the net capacitance associated with the system), that was superimposed on the trailing edge of the applied pulse. The system used two pairs of Ag-AgCl electrodes. One of these pairs was connected to a differential amplifier and served to measure voltage across the bilayer. The other served to apply voltage pulses across the bilayer and measure transmembrane current. The voltage source consisted of a programmable waveform synthesizer board WSB100 (Quatech Inc., Akron, OH) interfaced to an IBM-PC-compatible computer.

Before a membrane was pulsed, its specific capacitance ($C_{sp} = C_m/A_m$) was estimated. The method for measuring membrane capacitance exploited the fact that the intrinsic membrane resistance was at least two orders higher than the external resistance (R_e). Therefore, the time constant of voltage discharge was given by $\tau = R_eC$, which when measured could give an estimate of C. The membrane capacitance (C_m) was measured as follows. The solution level in the two compartments of the chamber was maintained just below the hole, and the time constant ($\tau = RC$) for the voltage decay through the external 1-MΩ resistance (R_e in Fig. 1) was measured by applying a low-amplitude (~100 mV), 10 μs, subthreshold rectangular voltage pulse. This time constant was used to compute total stray capacitance, ($C_s = C_T + C_b$) associated with the system, where C_T was the capacitance of the submerged Teflon sheet and C_b was the stray capacitance due to the circuit board, connectors, etc. Refer to Fig. 2 for an equivalent circuit of our experimental setup. The solution level in the two compartments of the chamber was then gradually raised to just above the hole to form a membrane, and the time constant for a subthreshold pulse was again measured. This second time constant was used to compute the net capacitance ($C_n = C_m + C_s$) associated with the system, where C_m was the membrane capacitance. Membrane capacitance (C_m) was estimated as $C_n - C_s$. This method offered a resolution of ~2 pF for capacitance measurement. The estimate for membrane capacitance also included a component equal to the incremental capacitance of the Teflon sheet (~5 mm^2 increase in area), which was submerged on raising the solution level above the hole. Assuming a dielectric constant of ~2 for Teflon, this contributed ~3 pF, which was small compared to typical membrane capacitance of 50 pF.

The area of the membrane (A_m) was assumed to be equal to the area of the hole, which was estimated by acquiring its image in a computer using an inverted microscope assembly and the imaging software IPLab (Signal Analytics Corp., Vienna, VA). This information, along with an estimate of total membrane capacitance (C_m), was used to calculate the specific capacitance of the membrane ($C_{sp} = C_m/A_m$).

The charge pulse and voltage clamp protocols were used to investigate the effect of poloxamer 188 (BASF, Parsippany, NJ) pretreatment on membrane electroporation. The two protocols are described in detail in the subsequent section. For both protocols, membranes electroporated irreversibly when exposed to a pulse of threshold amplitude. Therefore, the same membrane could not be used twice for obtaining the control information and to study the effect of poloxamer. In order to make a statistical comparison, experiments were performed on a large number ($n = 72$) of bilayers. Some of these membranes were used as control and the remaining were treated with poloxamer 188. In a single experimental session, approximately four to six membranes were formed. The first two or three of these membranes were used as control, and the later set (of two or three) was treated with poloxamer 188. Poloxamer was added to the bilayer chamber after the formation of a membrane, and its final concentration was adjusted at ~1.0 mM, close to its critical micelle concentration (CMC). Membranes were pulsed approximately 5 min after poloxamer 188 was added to the bilayer chamber.

Experimental protocols

A charge pulse experiment involved the rapid (few ns to μs) charging of a lipid membrane to some initial voltage (V_m), equivalent to depositing a charge $Q_m = C_mV_m$ on the membrane. This was followed by observing the decay in the transmembrane voltage as the membrane charge relaxed through an external resistance (R_e). The transmembrane voltage decay, which followed a relatively slow exponential time course for an intact

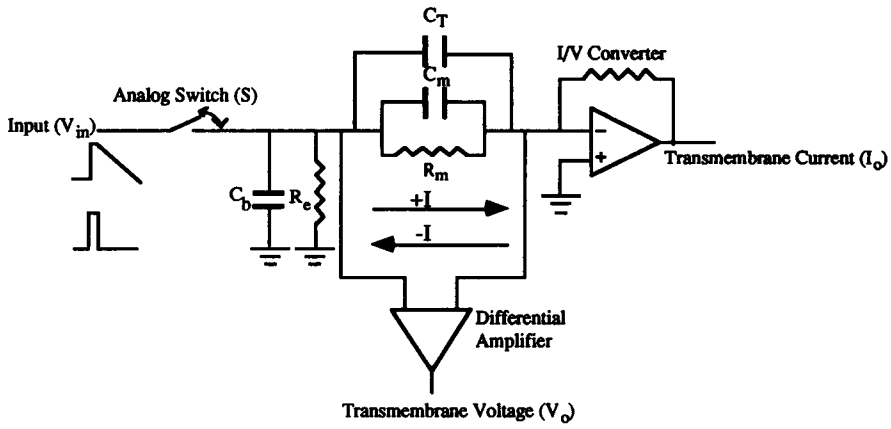

FIGURE 2 Equivalent circuit of the experimental setup. Teflon capacitance (C_T) appeared in parallel with membrane capacitance (C_m). Also, stray capacitance (C_b) due to board, connectors, etc. appeared effectively in parallel with C_m because the inverting terminal of the *I/V* (current to voltage) converter was virtually grounded. Arrows indicate the sign convention used for transmembrane current measurement. Transmembrane voltage and current were used to compute time course of membrane conductance ($G_m(t)$).

membrane, was greatly enhanced upon membrane electroporation because the high conductance of an electroporated membrane shunted the membrane charge. For a charge pulse experiment the time course of membrane conductance, which reflected the pore(s) dynamics, was computationally inferred from the transmembrane voltage. With this approach membrane conductance could be monitored only for a maximum of 100–150 μs (the time it took for the transmembrane voltage to decay to zero), whereas the changes in membrane conductance could last for several ms during irreversible electroporation. The duration for which membrane conductance could be monitored was extended by using the voltage clamp method, at the expense of increased circuit complexity. In this method transmembrane voltage could be controlled as desired, and the transmembrane current was simultaneously monitored. The transmembrane current, which increased several orders in magnitude upon membrane electroporation, could be used along with the transmembrane voltage to compute membrane conductance. The specific details of the two protocols in our experiments are given below.

Charge pulse

For charge pulse experiments (for a typical trace of the pulse protocol, see Fig. 3, panel *A*) the analog switch S (Fig. 1) was turned on for a duration of 10 μs, and a rectangular waveform of a desired amplitude was applied at the input of the switch. The switch was turned off synchronously with the end of the pulse and the decay of membrane voltage was observed through the external 1-MΩ resistance (R_e). The amplitude of the applied rectangular pulse was raised gradually from an initial value of ~100 mV in steps of ~5 mV until membrane electroporated irreversibly. This voltage was termed as threshold voltage. A delay of ~15 s was given between the two successive pulses. This protocol enabled us to probe the threshold voltage for membrane electroporation with a very high degree of accuracy. The onset of membrane electroporation was manifested as a decrease in the time constant of transmembrane voltage decay (for a typical trace see Results, Fig. 6).

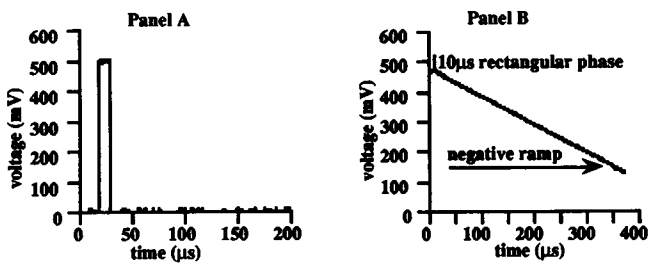

FIGURE 3 Voltage waveforms used for charge pulse (panel *A*) and voltage clamp (panel *B*) experiments. For a charge pulse experiment a rectangular 10 μs pulse of varying amplitudes was applied at the input of the analog switch (S in Fig. 1). After this the switch was turned off and transmembrane voltage decay was observed through an external 1 MΩ resistance (R_e). For a voltage clamp experiment the switch (S) was turned on for the entire duration of the waveform which consisted of an initial rectangular phase followed by a ramp of negative slope. The slope of the ramp was adjusted such that the voltage decayed to 0 mV in subsequent 500 μs.

Voltage clamp

In the voltage clamp experiments (Fig. 3, panel *B*) the analog switch (S) was turned on for the entire duration of 510 μs of the applied waveform. The first 10 μs of this total duration constituted an initial rectangular phase, referred to as the electroporating pulse or phase. In the subsequent 500 μs, transmembrane voltage decayed linearly to zero to constitute a negative-sloped ramp. The slope of the ramp was adjusted so that the transmembrane voltage decayed to zero mV at 500 μs irrespective of the amplitude of the initial rectangular phase. Such a pulse protocol allowed us to study the time course of membrane electroporation for a longer duration (500 μs) compared to ~150 μs for the charge pulse experiments, while maintaining a decay profile qualitatively similar to that observed with a charge pulse experiment. The amplitude of the rectangular phase is referred to as the clamp voltage. The threshold for irreversible electroporation was probed by incrementing the initial clamp voltage in steps of ~5 mV. For subthreshold pulses membrane conductance was very low, and the transmembrane current was purely capacitive. An upper bound of the capacitive current during the negative ramp, corresponding to the largest possible net capacitance (C_n) associated with the system, was estimated as $C_n[dV_m(t)/dt]$, and was found to be small (~0.05 μA) compared with the resolution (~0.1 μA) of our system. The onset of membrane electroporation was manifested as an increase in transmembrane current (for typical trace see Results, Fig. 8).

Transmembrane voltage and current were simultaneously recorded using a Tektronix 2211 digital storage oscilloscope. The data were then transferred to an IBM-PC-compatible computer via an RS-232 interface, and the ratio of current to voltage was used to compute membrane conductance [$G_m(t) = I_m(t)/V_m(t)$].

Statistical analysis

The statistical significance of changes in electroporation-related parameters for the control and poloxamer-treated membranes was determined using the nonparameteric Mann-Whitney test, a test most suitable in situations where the sample data cannot be assumed to follow a normal distribution (Zar, 1984). The *p*-values of less than 0.05 were considered significant for rejection of the null hypothesis.

RESULTS

Conductance of the bare hole

Fig. 4 shows the computed conductance of a bare hole (i.e., lipid-free, but aqueous-filled) obtained by applying a voltage clamp waveform with clamp voltage of ~500 mV across the Teflon sheet. As expected, the conductance is constant with a value of ~100 μS. The postelectroporation membrane conductance asymptotically approached this value. This will be elaborated in the section reporting results from the voltage clamp experiments.

Membrane capacitance

Membrane capacitance versus transmembrane voltage

Fig. 5, panel *A* shows the typical time course of transmembrane voltage decay for a subthreshold electroporation pulse, using the charge pulse protocol. Panel *B* shows a semilog plot of the same decay, which was found to have an R value of 0.997 for a linear fit. This implies that the transmembrane voltage decay was purely monoexponential, suggesting that membrane capacitance remained unaltered with changing transmembrane voltage.

Membrane specific capacitance

The specific capacitance of control (n = 36) and poloxamer treated (n = 36) membranes was measured to be 0.59 ± 0.21 μF/cm^2 and 0.66 ± 0.22 μF/cm^2, respectively [mean (μ) ± SD (σ)]. The assumption that the area of the membrane was equal to the area of the hole may have resulted in an underestimation of the membrane specific capacitance, since part of the hole was occupied by a relatively thick membrane supporting torus. Despite this, these values were found to be in good agreement with the range of specific capacitance reported for artificial lipid membranes (White and Thompson, 1973). Variation in unaccounted Teflon capacitance due to differences in solution level when raised above the hole (as discussed in Materials and Methods) could be a source of observed scatter in the measured specific capacitance.

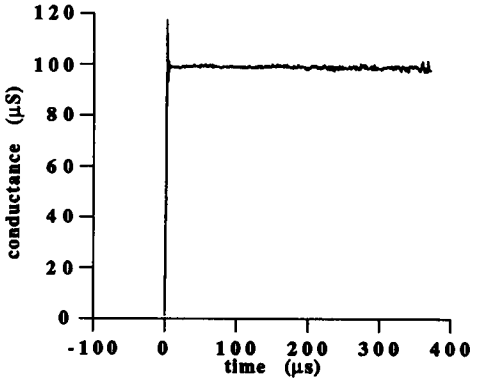

FIGURE 4 The conductance of a bare hole computed from transmembrane current and voltage following a voltage clamp protocol. As is clear, it is constant with a value of ~100 μS.

Effect of poloxamer 188 on capacitance of the same bilayer

To study the direct effect of poloxamer 188 on membrane capacitance, the change in membrane capacitance (n = 5) was monitored before and after the addition of poloxamer 188 (at 1.0 mM) to the bilayer chamber, without exposing the membrane to an electroporating pulse. We found that on addition of poloxamer 188, membrane capacitance showed ~4-8% decrease in approximately 5 min.

Charge pulse experiments

Typical membrane electroporation for a charge pulse experiment

Fig. 6 shows transmembrane voltage traces for a typical charge pulse experiment. V_1, V_2, and V_3 show the membrane voltage for subthreshold pulses, and V_4 the same on application of an electroporation-inducing threshold pulse. For a threshold pulse, the transmembrane voltage decay began with a subthreshold time constant (143.7 μs, for the trace shown in Fig. 6). After a variable interval from the end of the electroporating pulse (termed as latency time), an abrupt decrease in time constant (to 47.8 μs), attributable to an increase in membrane conductance upon electroporation, was observed. The degree of membrane poration was inferred by measuring the PEτ defined as the time for transmembrane voltage to decay by 63% from its value at the instant of initiation of electroporation (Fig. 7). Note that transmembrane voltage after membrane electroporation was not monoexponential. In this sense, 63% was arbitrary.

Effect of poloxamer 188 on membrane electroporation

The mean (μ) and standard deviation (σ) for threshold voltage, latency time, and PEτ for 10 control and 13 poloxamer 188-treated membranes are shown in Table 1. It is clear from these data that poloxamer-treated membranes showed higher mean threshold voltage (control: μ = 423.4 mV, poloxamer: μ = 448.4 mV, p = 0.1) and statistically significant, longer latency time (control: μ = 2.4 μs, poloxamer: μ = 19.0 μs, p = 0.04); and longer PEτ (control: μ = 11.6 μs, poloxamer: μ = 23.2 μs, p = 0.005).

Voltage clamp experiments

Typical membrane electroporation for a voltage clamp experiment

Fig. 8 shows the subthreshold (subscripts 1 and 2) and threshold (subscript 3) voltage, current, and conductance traces for a typical voltage clamp experiment. As discussed in Materials and Methods, the subthreshold transmembrane

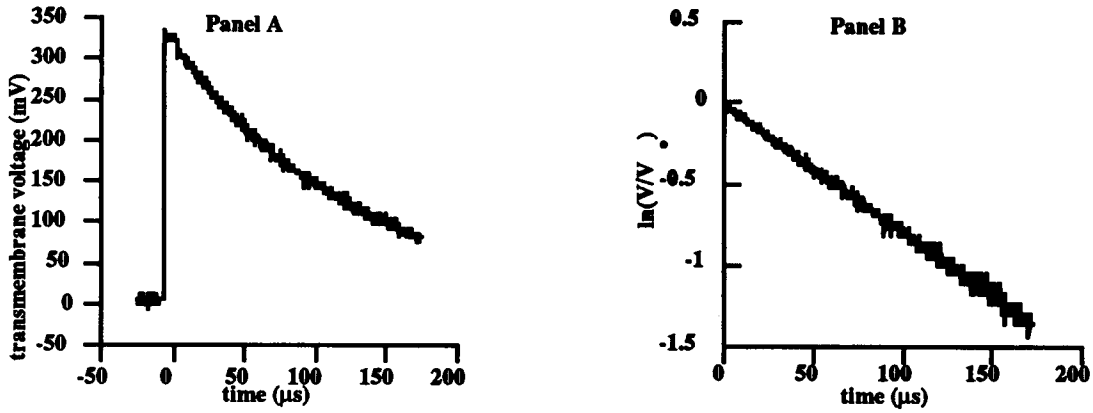

FIGURE 5 Panel A shows capacitive discharge of a membrane for a subthreshold pulse and panel B shows the same on a semi-log plot. The semi-log plot had an excellent linear fit (R = 0.997) suggesting that the voltage decay was mono-exponential. This implies that the membrane capacitance, and therefore membrane thickness, were independent of transmembrane voltage.

current (I_1 and I_2) was small compared to the resolution of our system and, therefore, lay close to zero. For a threshold pulse, the transmembrane current had a typical time course as shown by I_3. A variable latency time, as in the case for charge pulse experiments, was observed. Fig. 8, panel *C* shows the computed membrane conductance (G_m). For reference, the conductance of the bare hole (G_{ref}) is also shown in the same panel. In order to ascertain the time required for complete rupture of a membrane (~100 μm in diameter) following a threshold pulse, membrane electroporation was recorded over a longer time scale (Fig. 8, panel *D*). The membrane conductance recorded at a higher temporal resolution (Fig. 8, panel *C*) exhibited two phases. This was evident from the fact that the best fit for this trace of membrane conductance was obtained by equation $G_m = G_{o1}(1 - e^{-t/\tau 1}) + G_{o2}(1 - e^{-t/\tau 2})$. Values for the time constant τ_1 and τ_2 were found to be 25 μs and 1750 μs, respectively (with G_{o1} = 20 μs and G_{o2} = 90 μs). The membrane conductance recorded over an even longer time scale (Fig. 8, panel *D*) began to increase more slowly when it approached the reference conductance. This may be considered as an additional third phase in the membrane conductance dynamics and could be a result of the membrane supporting torus retarding the process of membrane rupture in its final stages.

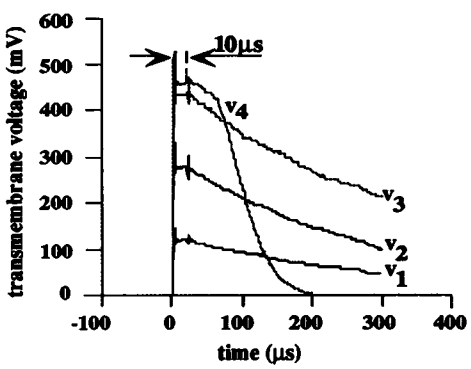

FIGURE 6 Transmembrane voltage traces for a typical charge pulse experiment. V_1, V_2, and V_3 show transmembrane voltage for subthreshold pulses and V_4 for a threshold pulse. Membrane electroporation is manifested as an increase in rate of transmembrane voltage decay.

Effect of poloxamer 188 on membrane electroporation

The threshold voltage, latency time, and membrane conductance (200 μs after the onset of electroporation) for 26 control and 23 poloxamer-treated membranes are compared in Table 1. These data clearly show that poloxamer 188 modifies a membrane so as to increase its threshold voltage (control: μ = 442 mV, poloxamer: μ = 509 mV, p = 0.06) for irreversible electroporation. Also, poloxamer 188 treatment prolonged the latency time (control: μ = 10 μs, poloxamer: μ = 35 μs, p = 0.05) and decreased the postelectroporation conductance (control: μ = 41 μS,

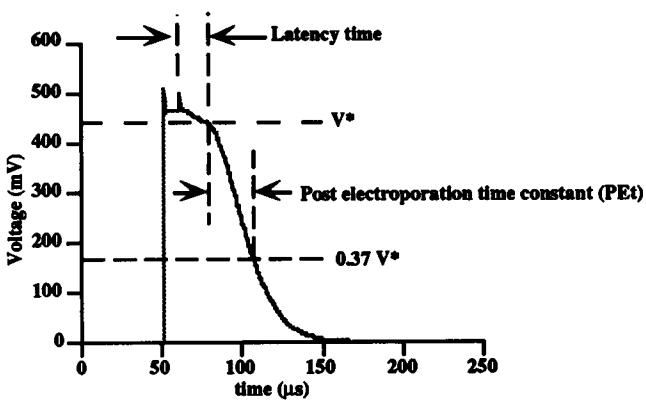

FIGURE 7 Terminology used in the text for a charge pulse experiment. Latency time was measured from the end of a 10-μs electroporating pulse to the onset of electroporation. PEτ (postelectroporation time constant) quantified the extent of membrane electroporation and was defined as the time for transmembrane voltage to decay by 63% from the instant of initiation of electroporation (at voltage V*).

TABLE 1 Comparison of mean (μ) and standard deviation (σ) of electroporation-related parameters for charge pulse and voltage clamp protocols

	Charge pulse					Voltage clamp				
	Control (10)		Poloxamer-treated (13)			Control (26)		Poloxamer-treated (23)		
	μ	σ	μ	σ	p	μ	σ	μ	σ	p
Threshold voltage (mV)	423.4	29.4	448.4	87.6	0.1	441.6	23.2	509.2	139.0	0.06
Latency time (μs)	2.4	5.3	19.0	22.1	0.04	9.9	15.3	35.2	44.8	0.05
Membrane conductance (μS)	—	—	—	—	—	40.8	14.7	28.4	16.3	0.001
PEτ (μs)	11.7	3.8	23.2	8.2	0.005	—	—	—	—	—
Rise time (t_r) (μs)	—	—	—	—	—	36.7	24.5	61.4	41.9	0.05

The numbers in parentheses indicate the number of membranes used for experiments in each category. The p-value indicated against each parameter is the significance level with which null hypothesis can be rejected for the corresponding parameter.

poloxamer: μ = 28 μS, p = 0.001). The increase in threshold voltage and latency time, and decrease in postelectroporation conductance, for poloxamer-treated membranes are consistent with the results obtained from charge pulse experiments. We also quantified the rate of increase of membrane conductance at the onset of electroporation by estimating the time required by conductance to reach a value of $0.33G_{ref}$ (Fig. 8, panel *C*). This was termed as rise time (t_r). The mean rise time for control and poloxamer-treated membranes are compared in Table 1. Poloxamer 188-treated membranes showed a longer t_r at the onset of electroporation.

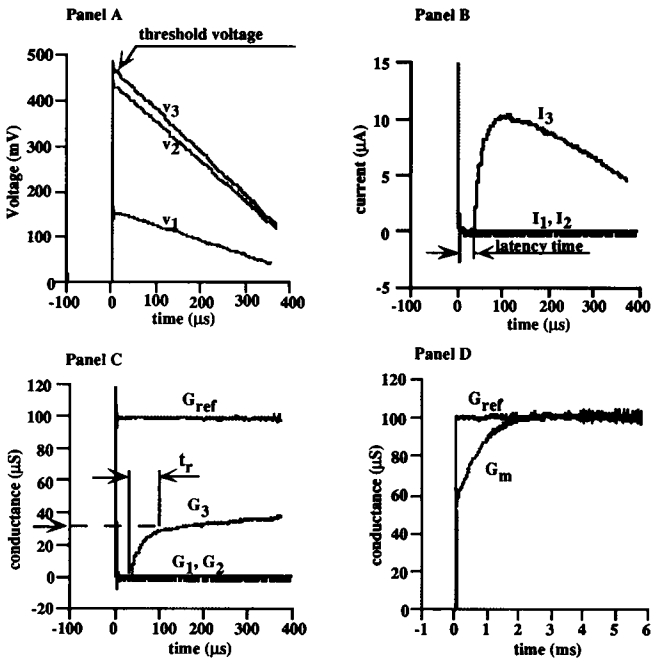

FIGURE 8 Typical voltage (panel *A*), current (panel *B*) and conductance (panel *C*) traces for a voltage clamp experiment. For subthreshold voltage pulses (V_1 and V_2) the corresponding transmembrane current (I_1 and I_2) is ~0, and so is the computed conductance (G_1 and G_2). For an electroporation-causing threshold pulse (V_3), I_3 and G_3 are the corresponding transmembrane current and conductance traces. In panel *C*, the arrowhead on the conductance axis corresponds to a value of 0.33 G_{ref}, which is used to estimate the rise time for membrane conductance. Panel *D* shows the membrane conductance (G_m) on application of a voltage clamp waveform for which negative ramp (following initial 10 μs rectangular phase) was 8 ms long. The membrane conductance can be seen to approach reference conductance (G_{ref}) for a bare hole.

Comparison between charge pulse and voltage clamp experiments

The time course of membrane conductance during a charge pulse experiment could be computed assuming that the membrane capacitance (C_m) remained constant during electroporation (Appendix A). This assumption was valid at least during the first 500 μs of membrane electroporation because, as discussed earlier, it took approximately an order of magnitude longer for complete rupture of the membrane to occur. A typical estimated time course of membrane conductance for a charge pulse experiment is shown in Fig. 9 along with a voltage clamp conductance trace. Both experiments yielded similar time courses of membrane conductance; however, the voltage clamp experiments had an obvious advantage in terms of the duration over which membrane conductance could be monitored. A careful inspection of Table 1 reveals that the mean latency time and threshold voltage for voltage clamp experiments were higher compared to those for charge pulse experiments. The significance of this finding will be discussed shortly.

DISCUSSION

In this study of artificial lipid membranes made of azolectin, we found that poloxamer 188 had a significant effect on electroporation-related parameters. Threshold voltage, latency time, t_r, and PEτ all showed an increase; whereas membrane conductance (measured 200 μs after the onset of electroporation) showed a decrease. The mean threshold voltage for poloxamer-treated membranes was found to be 25 mV higher in the charge pulse experiments and 67 mV higher in the voltage clamp experiments. This corresponds to a ~6% and 15% increase in threshold voltage for poloxamer 188-treated membranes compared to the control membranes for the charge pulse and voltage clamp experiments,

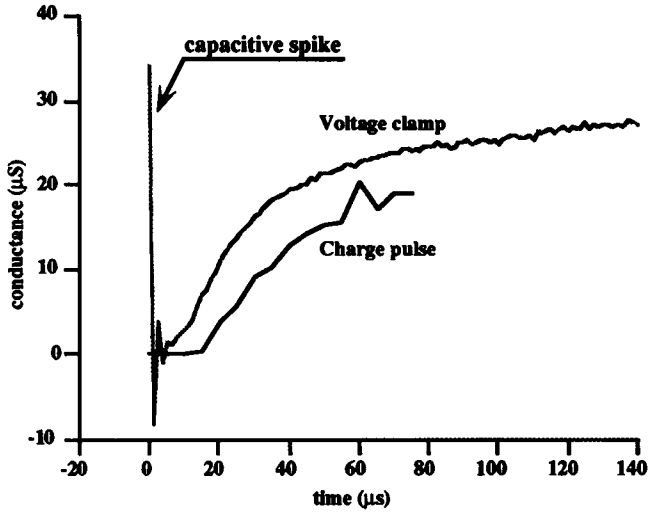

FIGURE 9 Comparison of time course of membrane conductance for a voltage clamp and charge pulse experiment. Membrane conductance showed the same trend for both experimental protocols. The large spike at the beginning of voltage clamp conductance is due to capacitive current. A voltage clamp experiment had the obvious advantage of allowing the membrane conductance to be monitored for a much longer duration compared to a charge pulse experiment.

respectively. The mean latency time for poloxamer-treated membranes was found to be 17 μs longer for charge pulse experiments and 25 μs longer for voltage clamp experiments. This corresponds to a ~700% and 250% increase in latency time for poloxamer 188-treated membranes compared to the control membranes for the charge pulse and voltage clamp experiments, respectively. The membrane conductance decreased by 12.4 μS (~30%) and t_r increased by 25 μs (~67%) for poloxamer-treated membranes. Together, these findings suggest that poloxamer decreases the susceptibility of lipid membranes to electroporation. Also, the PEτ was found to increase by ~12 μs, a 100% increase, for poloxamer-treated membranes. This result is consistent with the lower level of membrane conductance of poloxamer-treated membranes after electroporation. Although the two protocols led to the same qualitative conclusion, the mean threshold voltage and latency time for the two protocols were found to be different. A possible source of these differences is discussed below.

Charge pulse versus voltage clamp

The mean threshold voltage and latency time for both the control and poloxamer-treated membranes were lower for charge pulse experiments than for voltage clamp experiments (Table 1). The p-values for rejection of equal mean hypothesis for threshold voltage and latency time were found to be 0.1 and 0.2, respectively, for control membranes, and 0.1 and 0.5, respectively, for poloxamer-treated membranes. Although the slope of the ramp used in the voltage clamp protocol was chosen to be longer than the postelectroporation time constant, it generally was faster than the decay rate of membrane voltage in the charge pulse experiment before membrane breakdown. This implies that, for an electroporating pulse of the same intensity, membranes were exposed to a higher voltage during a charge pulse experiment compared to a voltage clamp experiment at comparable time intervals before breakdown. Benz and Zimmermann (1980) studied the effect of pulse length on threshold voltage for electroporation in lipid membranes made of oxidized cholesterol, and found that the threshold voltage decreased with an increase in pulse duration. Abidor et al. (1979) studied electroporation in artificial lipid bilayers and found that the latency time decreased with an increase in intensity of applied pulse. In light of these findings, the inter-protocol differences in threshold voltages and latency times observed by us can be readily explained. A slower decay of transmembrane voltage for charge pulse experiments is analogous to a longer effective pulse duration and higher effective pulse intensity.

Membrane capacitance and conductance

Membrane capacitance

Our findings of voltage independence of membrane capacitance are consistent with that of Alvarez and Latorre (1978) who used a very sensitive assay and showed that voltage-dependent changes in capacitance of membranes formed using folding method range from 0.01% to 1.0%. The capacitance change under the influence of an externally imposed field directly reflects a change in average thickness of the membrane. Thus, the voltage independence of membrane capacitance for poloxamer-free membranes implies that the average thickness of our membranes did not change under the influence of the applied field. Chernomordik et al. (1982) showed that for UO_2^{2+}-modified artificial lipid bilayers, even on application of transmembrane voltage of ~700 mV, large compared to ~150 mV used for capacitance measurement in our experiments, very little (<2%) change in membrane capacitance was observed.

Membrane conductance

Electroporation in artificial lipid membranes has been studied in considerable detail by Zimmermann and colleagues using the charge pulse method, and Chernomordik and colleagues using the voltage clamp method. For example, refer to Benz et al. (1979) and Chernomordik et al. (1983). From the rapid decay of postelectroporation transmembrane voltage traces, Benz et al. inferred that membrane resistance for bilipid membranes made from oxidized cholesterol decreased by ~8 orders of magnitude in less than 100 ns upon electroporation. However, they did not explicitly compute the membrane conductance. Chernomordik et al. studied the electroporation of membranes made from oxidized cholesterol and UO_2^{2+}-modified azolectin using the voltage clamp method. They report that on exposure to ms duration pulses, irreversible electroporation, as manifested by an abrupt

jump in transmembrane current, was preceded by a slow and reversible increase in transmembrane current. The focus of their study was primarily the initial slow phase of the membrane electroporation. This difference in focus, along with differences in the time scale of operation, prevents a direct comparison of their membrane conductance results to ours.

The biphasic behavior of conductance of our planar artificial membranes after electroporation bears a resemblance to that observed for a suspension of erythrocytes in isotonic saline by Kinosita and Tsong (1979). They observed a conductance increase with a rapid (~1 μs) phase followed by a slow (~100 μs) phase upon application of an electric field above a threshold value (~1.5 kV/cm). Our estimates of the time scale of the two phases (25 μs and 1750 μs) are an order of magnitude slower than theirs. This may be attributed to the morphological and structural differences between erythrocytes and lipid bilayers. Despite the differences in time scale estimated by us and Kinosita and Tsong, in both studies the second phase is an order of magnitude slower than the first, and may reflect a similar sequence of events underlying electroporation. Kinosita and Tsong's interpretation was that the first phase reflected the formation of aqueous pores and second phase reflected their slow expansion, a hypothesis that remains reasonable in light of our results. The similarity of results obtained from lipid bilayers to those obtained from cell membranes strongly supports the reasonably well established hypothesis that electroporation occurs mainly in the lipid matrix of the cell membranes.

Possible mechanisms of membrane-poloxamer interaction

Interaction between poloxamer 188 and a lipid monolayer

Among several model systems used to study physico-chemical properties of biological membranes, lipid monolayers have the advantage of being experimentally the most flexible (Cadenhead, 1985). They are formed by depositing a lipid dissolved in an organic solvent on an aqueous-gas interface. The organic solvent evaporates, leaving behind the adsorbed lipid. By sweeping a barrier along the interface, the area per molecule of the lipid can be controlled, allowing the monolayer to be studied in a variety of surface states, analogous to fluid and condensed states of a bilayer.

Consider a monolayer spread on the interface of a solution containing a soluble surfactant. The adsorption of the surfactant can be inferred by studying the surface pressure [surface tension reduction; surface pressure (π) = surface tension of water (γ_{water}) − surface tension of monolayer ($\gamma_{monolayer}$)], which increases as the surfactant adsorbs. The interaction of a soluble, macromolecular surfactant such as poloxamer with an insoluble monolayer has drawn considerable attention from theoreticians (de Gennes, 1990) and experimentalists alike. The experimental findings demonstrate that the surface pressure depends on the molecular structure of the insoluble component (Lee et al., 1993; Maget-Dana and Ptak, 1995), its surface concentration (Magalhaes et al., 1991; Weingarten et al., 1991) as well as on the structure (Ah-Fat et al., 1994) and bulk concentration (Magalhaes et al., 1991; Weingarten et al., 1991) of the soluble surfactant.

Poloxamer 188 contains a central hydrophobic core consisting of ~30 units of propylene oxide (PO) and two flanking hydrophilic chains, each consisting of ~75 units of ethylene oxide (EO). The hydrophobic PO repeat units probably adsorb to intercalate among the hydrocarbon tails of the lipid at the interface, leaving the flanking EO repeat units immersed in the aqueous phase. Weingarten et al. (1991) studied the interaction of poloxamer 188 with phosphatidycholine monolayers. In their experiments (as reported in their Fig. 4) lipid was spread on an aqueous poloxamer 188 solution and dynamically compressed. When compared to poloxamer-free systems, the surface pressures were higher and, for low surface pressures (corresponding to expanded monolayers), increased monotonically with bulk concentration of the poloxamer. At higher surface compression (corresponding to more densely packed lipid monolayers) the surface pressures were still in excess of the poloxamer-free system, but approached each other in a manner consistent with the "squeezing out" of some of the adsorbed poloxamer.

The behavior of the monolayer differed above and below the critical micelle concentration (CMC). Above the CMC, the surface pressures were consistently higher and were relatively insensitive to changes in the bulk concentration of poloxamer over an order of magnitude. In addition, while below the CMC the monolayers could be compressed to a critical surface pressure (the collapse pressure) that was roughly equal to the poloxamer-free membrane, above the CMC all monolayers had the same collapse pressure that was higher than the poloxamer free value. In all cases, the monolayer could be compressed to a similar final area/molecule that was roughly equal to that of the lipid, indicating that much of the adsorbed poloxamer may be ejected from the monolayer during compression.

Weingarten et al. (1991) suggest that the increase in collapse pressure observed above the CMC may be caused by the alignment of poloxamer 188 next to the lipid monolayer, mediated by favorable interactions between the lipid headgroups and the EO groups of a poloxamer molecule. Such an associated layer could strengthen the monolayers against collapse.

Magalhaes et al. (1991) also studied the interactions of poloxamer 188 with phosphatidylcholine monolayers. In their experiments, an insoluble monolayer was spread on the interface of an aqueous poloxamer solution, and the equilibrium surface pressure was studied as a function of initial lipid surface pressure and poloxamer concentration. They found that surface pressures *greater than* the surface tension reduction caused by the poloxamer alone were realized for expanded lipid monolayers, and *less than* the surface tension reduction for condensed monolayers. This is consistent

with an increasing energy barrier to adsorption caused by cohesive interactions among the lipid molecules (Sundaram and Stebe, 1996).

These studies clearly show that poloxamer 188 can adsorb into insoluble monolayers and change their mechanical behavior in a manner that depends on the initial state of the monolayer and the concentration of poloxamer in solution (which has an impact on the adsorbed state of the poloxamer).

Similar changes may occur in bilayer membranes; de Gennes (1990) discusses the effects of polymer adsorption on bilayer membrane mechanical properties. For example, he gives scaling arguments for the increase in membrane viscosity and elasticity caused by polymer adsorption, showing that this increase depends on the number of monomer repeat unit between "entanglements" (which can correspond to sites along a poloxamer molecule where the PO groups have adsorbed to intercalate between the lipid molecules). As the number of monomers free to move between entanglements decreases, the membrane viscosity and elastic modulus increases. An increase in membrane viscosity should slow its morphological response to critical stresses. This has clear implications in the prolonged time scales for electroporation onset of poloxamer-treated membranes observed in our study, and supported by others, as is discussed further below.

Existing evidence for bilayer-poloxamer interaction

Evidence for poloxamer 188 interaction with lipid bilayers is available from studies with liposomes, erythrocytes, and artificial bilipid membranes. Treatment of liposomes with poloxamer-like surface active agents is known to decrease their hemolytic activity toward erythrocytes (Quirion and St-Pierre, 1991) and inhibit lysis of erythrocytes themselves in a hypotonic environment (Gaehtgens and Benner, 1973). These authors have proposed adsorption of poloxamer into the membranes of liposomes and erythrocytes as the underlying mechanism to explain their observations.

Membrane conductance during electroporation, with and without poloxamer, has been studied by Benz and collaborators. Wilhelm et al. (1993) inferred that, for a poloxamer-free system, the membrane conductance increased linearly with a slope of ~0.3S/s during the irreversible breakdown of a lipid membrane following a charge pulse protocol. Our results confirm and extend their finding. During the initial 10's of μs (the measurement interval of Wilhelm et al.) we also find a linear increase in conductance, with a slope of ~0.5 S/s. However, the growth in conductance slows in a biphasic fashion during the following 350 μs. In another study from the same group, Klotz et al. (1993) studied the effect of several different macromolecules, among them poloxamer 188, on irreversible electroporation of planar lipid membranes. They found that membranes exposed to poloxamer 188 solution had a lower linear rate of conductance increase during irreversible membrane electroporation compared to poloxamer-free membranes. This was attributed to a strong binding affinity of poloxamer 188 for the membrane, which increased the membrane inertia and slowed the rate of expansion of what was they presumed to be a single pore. The increased t_r for our poloxamer-treated membranes is consistent with a slower pore growth rate but, at the present time, we cannot say with any certainty if the membrane conductance reflects the growth of a single large pore or of several small pores.

Poloxamer-induced changes in the membrane

Analogous to a monolayer, the state of a bilayer can be expected to be an important factor in determining the mechanism of bilayer-poloxamer interaction. If the bilayer is in a fluid state, where the lipid molecules are loosely packed and average intermolecular distances are large, poloxamer may be easily incorporated into the membrane. If, on the other hand, the bilayer is in a condensed state, poloxamer molecules may be excluded from the bilayer and interact primarily by forming an associated layer in the subphase adjacent to the solution-facing surfaces of the membrane. Either mechanism will increase the effective membrane thickness. This change in thickness has implications in terms of the membrane capacitance; thicker membranes have smaller capacitance. This is consistent with our findings of an ~4% to 8% decrease in the capacitance of the poloxamer-treated membranes. Assuming that the membrane area remained constant on addition of poloxamer, for a membrane with initial thickness of 70 Å, a 4–8% decrease in membrane capacitance corresponds to a 4–8-Å thick adsorbed layer of poloxamer on either face of the membrane. Poloxamer adsorbed into the two faces of the membrane acts as a pair of capacitors [specific capacitance (C_p) of ~2.2–4.4 μF/cm^2 assuming a dielectric constant of ~2 for poloxamer] in series with the membrane capacitance (typically 0.5 μF/cm^2). Assuming that the intrinsic threshold voltage for a membrane does not change significantly in the presence of poloxamer, this will cause an 18–30% increase in threshold voltage, a range consistent with our experimental findings. The lower conductance (refer to Table 1) for the poloxamer-treated membranes after electroporation can be envisioned to be the result of an ability of adsorbed poloxamer layers to limit the size and number of pores formed in the membrane.

In addition to the effective thickness, the chemical composition of a membrane is also altered by poloxamer. The insertion of poloxamer PO groups into a membrane may decrease the effective dielectric constant of the membrane, which may decrease the membrane capacitance. However, because the dielectric constant of the hydrophobic core of the membrane (~2) is itself very low, this effect will probably be slight. The capacitance decrease observed in our system showed some variability. Recall that the total amount of poloxamer adsorbed into a bilayer depends on the bilayer state. Because the state of a membrane formed by the folding method cannot be controlled, it is possible that

there were differences in the degree of fluidity from one membrane to another, which could be a source of the variable decrease in capacitance observed for the five membranes we studied.

Implications

Lee et al. (1992), indeed, found that the postshock decrease in the impedance of their experimental muscle flap was reduced in a dose-dependent manner by pretreatment with poloxamer 188; a higher dose resulting in a smaller impedance drop. Moreover, the impedance recovery rate was faster for higher pretreatment doses. These investigators suggested that poloxamer may be able to dynamically plug the pores after their formation. Our findings offer an alternative explanation for their observations. The dose-response curve may be explained in terms of the decrease in the fractional area of porated cell membranes by poloxamer, owing to an increase in effective threshold voltage for electroporation. The reduction in drop of muscle impedance after electroporation may be explained to be a result of formation of smaller dimension pores with an increase in surface adsorption of poloxamer 188. The faster recovery of flap impedance may be due to formation of smaller pores that tend to close faster.

Several electroporation theories (Abidor et al., 1979; Weaver and Barnett, 1992) invoke membrane surface tension. According to these theories, energy of a pore of radius "a" in the absence of an external field is given by $E_{pore} = 2\pi a\gamma - \pi a^2\sigma$. Here, γ is the line tension of the pore and σ the surface tension of the membrane. The critical diameter of a pore is given by $a_c = \gamma/\sigma$. A pore with its radius below the critical radius "a_c" tends to close, whereas above it the pore will tend to grow irreversibly. If the surface tension of the membrane is lowered, the driving force [$F_{pore} = (d/da)E_{pore} = 2\pi(\gamma - a\sigma)$] for growth of a pore ($a > a_c$) decreases while for closure of a pore ($a < a_c$) increases. Also, the critical pore radius for irreversible membrane breakdown increases. Therefore, a lower surface tension of our poloxamer-treated membranes compared to control membranes may explain the observed increase in rise time (a slower growth of pores) and threshold voltage. A similar reduction in surface tension of the membranes pretreated with poloxamer and concomitant increase in threshold voltage may also explain a dose dependent drop in flap impedance (see above) as observed by Lee et al. (1992). Poloxamer 188 may also alter the line tension (γ) of electropores but no experimental data are currently available to test this hypothesis.

Needham and Hochmuth (1989), by performing micropipette aspiration experiments on lipid vesicles, showed that the treatment of vesicles with cholesterol alters the membrane elastic moduli and raises the threshold voltage for electroporation. A similar increase in elastic moduli of poloxamer-treated lipid membranes may offer an alternative explanation for the higher observed threshold voltage in our experiments.

Thus, modification of the surface properties of cell membranes by poloxamer 188 may significantly contribute toward decreasing the damage sustained by cells during the event of an electrical shock. This property of poloxamer, along with its nontoxic nature, makes it, or similar compounds, a potential candidate for the in vivo chemical treatment of tissues to reduce electrical shock-induced injury.

APPENDIX A

The time course of membrane conductance was obtained by dividing the membrane voltage decay into n equal intervals ($n = 14$) and assuming that transmembrane voltage decay followed a monoexponential time course given by $V(t) = V_{ko}e^{-t/\tau_k}$ (where V_{ko} and τ_k are, respectively, the maximum transmembrane voltage and time constant for voltage decay associated with the kth interval) in each of these intervals. τ_k dynamically changed from one interval to the next as membrane conductance [$G_m(t)$] changed. Also,

$$\tau_k = C_n(R_{mk} + R_e) \tag{A1}$$

Equation A1 can be rewritten as,

$$\tau_k = C_n\left(\frac{1}{G_{mk}} + \frac{1}{G_e}\right) \tag{A2}$$

where $G_{mk} = 1/R_{mk}$ is the membrane conductance, assumed to be approximately constant over the kth time interval, $G_e = 1/R_e$ is the conductance of the external resistor, and C_n = net capacitance (see Materials and Methods).

Equation A2 can be easily rearranged to give,

$$G_{mk} = \frac{C_nG_e}{\tau_kG_e - C_n} \tag{A3}$$

To compute G_{mk}, τ_k is required, which is calculated for the time at the beginning of each interval as,

$$\tau_k = \left[V(t)\frac{d}{dt}\left(\frac{1}{V(t)}\right)\right]^{-1} \tag{A4}$$

G_{mk} (k: 1, . . . , n) gives an approximation for the time course of membrane conductance $G_m(t)$.

We would like to thank Dr. Andrew Harris and members of his lab for the help extended during the initial phase of this work.

This work was supported by a Johns Hopkins Whiting School and Applied Physics Lab (APL) Research Initiation grant, an APL graduate fellowship (to V.S.), and by a grant from the National Institutes of Health (RO1 48266) (to L.T.).

REFERENCES

Abidor, I. G., V. B. Arakelyan, L. V. Chernomordik, Y. A. Chizmadzhev, V. F. Pastushenko, and M. R. Tarasevich. 1979. Electric breakdown of bilayer lipid membranes. I. The main experimental facts and their qualitative discussion. *Bioelectrochem. Bioenerg.* 6:37–52.

Ah-Fat, N. M. W., D. Q. M. Craig, and K. M. G. Taylor. 1994. An investigation into the effects of surfactants on phospholipid monolayers using Langmuir-Blodgett film balance. *Int. J. Pharm.* 107:239–242.

Alvarez, O., and R. Latorre. 1978. Voltage-dependent capacitance in lipid bilayers made from monolayers. *Biophys. J.* 21:1–17.

Belehradek, M., C. Domenge, B. Luboinski, S. Orlowski, J. Belelhradek, and L. M. Mir. 1993. Electrochemotherapy, a new antitumor treatment. First clinical phase I-II trial. *Cancer.* 72:3694–3700.

Benz, R., F. Beckers, and U. Zimmermann. 1979. Reversible electrical breakdown of lipid bilayer membranes: A charge-pulse relaxation study. *J. Membr. Biol.* 48:181–204.

Benz, R., and U. Zimmermann. 1980. Pulse-length dependence of the electrical breakdown in lipid bilayer membranes. *Biochim. Biophys. Acta.* 597:637–642.

Cadenhead, D. A. 1985. Monomolecular films as biomembrane models. *In* Structure and Function of Biomembranes, G. Benga, editor. CRC Press, Inc., Boca Raton, Florida.

Chalmers, R. A. 1985. Comparison and potential of hypo-osmotic and iso-osmotic erythrocyte ghosts and carrier erythrocytes as drug and enzyme carriers. *Bibl. Haematol.* 51:15–24.

Chernomordik, L. V., S. I. Sukharev, I. G. Abidor, and Y. A. Chizmadzhev. 1982. The study of the BLM reversible electrical breakdown mechanism in the presence of UO_{22+}. *Bioelectrochem. Bioenerg.* 9:149–155.

Chernomordik, L. V., S. I. Sukharev, I. G. Abidor, and Y. A. Chizmadzhev. 1983. Breakdown of lipid bilayer membranes in an electric field. *Biochim. Biophys. Acta.* 736:203–213.

Chizmadzhev, Y. A., V. B. Arkelyan, and V. F. Pastushenko. 1979. Electrical breakdown of bilayer membranes. III. Analysis of possible mechanisms of defect origin. *Bioelctrochem. Bioenerg.* 6:63–70.

Crowley, J. M. 1973. Electrical breakdown of bimolecular lipid membranes as an electrical instability. *Biophys. J.* 13:711–724.

de Gennes, P. G. 1990. Interactions between polymers and surfactants. *J. Phys. Chem.* 94:8407–8413.

Freeman, S. A, M. A. Wang, and J. C. Weaver. 1994. Theory of electroporation of planar bilayer membranes: predictions of the aqueous area, change in capacitance, and pore-pore separation. *Biophys. J.* 67:42–56.

Gaehtgens, P., and K. U. Benner. 1973. Inhibitory effect of non-ionic detergent on osmotic lysis of human red blood cells. *Eur. J. Physiol.* 343:R1.

Gaylor, D. C., D. L. Bhatt, and R. C. Lee. 1992. Skeletal muscle cell membrane electrical breakdown in electrical trauma. *In* Electrical Trauma: the Pathophysiology, Manifestation and Clinical Management. R. C. Lee, E. G. Cravalho, and J. F. Burke, editors. Univ. of Cambridge Press, Cambridge, UK.

Hong, S. C., G. Lanzino, Y. Goto, S. K. Kang, F. Schottler, N. F. Kassell, and K. S. Lee. 1994. Calcium-activated proteolysis in rat neocortex induced by transient focal ischemia. *Brain Res.* 661:43–50.

Hymes, A. C., H. J. Robb, and R. R. Margulis. 1970. Influence of an industrial surfactant (Pluronic F-68) on human amniotic fluid embolism. *Am. J. Obstet. Gynecol.* 107:1217–1222.

Johnston, T. P., and S. C. Miller. 1985. Toxicological evaluation of poloxamer vehicles for intramuscular use. *J. Parenter. Sci. Technol.* 39:83–89.

Kinosita, K., and T. Y. Tsong. 1979. Voltage-induced conductance in human erythrocyte membranes. *Biochim. Biophys. Acta.* 554:479–497.

Klotz, K. H., M. Winterhalter, and R. Benz. 1993. Use of irreversible electrical breakdown of lipid bilayers for the study of interaction of membranes with surface active molecules. *Biochim. Biophys. Acta.* 1147:161–164.

Kolodgie, F. D., A. Farb, G. C. Carlson, P. S. Wilson, and R. Virmani. 1994. Hyperoxic reperfusion is required to reduce infarct size after intravenous therapy with perfluorochemical (Fluosol-DA 20%) or its detergent component (poloxamer 188) in a poorly collateralized animal model. Absence of a role of polymorphonuclear leukocytes. *J. Am. Coll. Cardiol.* 24:1098–1108.

Kubiniec, R. T., H. Liang, and S. W. Hui. 1990. Effects of pulse length and pulse strength on transfection by electroporation. *Biotechniques.* 8:16–20.

Lee, L. T., E. K. Mann, O. Guiselin, D. Langevin, B. Farnoux, and J. Penfold. 1993. Polymer-surfactant films at the air-water interface. 2. A neutron reflectivity study. *Macromolecules.* 26:7046–7052.

Lee, R. C., A. Myerov, and C. P. Maloney. 1994. Promising therapy for cell membrane damage. *In* Electrical Injury: A Multidisciplinary Approach to Therapy, Prevention and Rehabilitation. R. C. Lee, M. Capelli-Schellpfeffer, and K. M. Kelley, editors. *Ann. N. Y. Acad. Sci.* 720: 239–245.

Lee, R. C., L. P. River, Fu-shih Pan, L. Ji, and R. L. Wollmann. 1992. Surfactant-induced sealing of electropermeabilized skeletal muscle. *Proc. Natl. Acad. Sci. USA* 89:4524–4528.

Magalhaes, N. S. S., S. Benita, and A. Baszkin. 1991. Penetration of poly(oxyethylene)-poly(oxypropylene) block copolymer surfactant into soya phospholipid monolayers. *Colloids Surf.* 52:185–206.

Maget-Dana, R., and M. Ptak. 1995. Interactions of surfactin with membrane models. *Biophys. J.* 68:1937–1943.

Maldarelli, C., and K. Stebe. 1992. An anisotropic, elastomechanical instability theory for electropermeabilization of bilayer-lipid membranes. *In* Electrical Trauma: the Pathophysiology, Manifestation and Clinical Management. R. C. Lee, E. G. Cravalho, and J. F. Burke, editors. Univ. of Cambridge Press, Cambridge, UK.

Mir, L. M., S. Orlowski, J. Belehradek, Jr., and C. Paoletti. 1991. Electrochemotherapy potentiation of antitumour effect of bleomycin by local electric pulses. *Eur. J. Cancer.* 27:68–72.

Mitsuno, T., H. Ohyanagi, and K. Yokoyama. 1984. Development of a perfluorochemical emulsion as a blood gas carrier. *Artif. Organs.* 8:25–33.

Needham, D., and R. M. Hochmuth. 1989. Electro-mechanical permeabilization of lipid vesicles. Role of membrane tension and compressibility. *Biophys. J.* 55:1001–1009.

Neumann, E., and K. Rosenheck. 1972. Permeability changes induced by electric impulses in vesicular membranes. *J. Membr. Biol.* 10:279–290.

Neumann, E., A. E. Sowers, and C. A. Jordan. 1989. Electroporation and Electrofusion in Cell Biology. Plenum Press, New York.

Okino, M., and H. Mohri. 1987. Effects of a high-voltage electrical impulse and an anticancer drug on in vivo growing tumors. *Jpn. J. Cancer Res. (Gann).* 78:1319–1321.

Padanilam, J. T., J. C. Bischof, R. C. Lee, E. G. Cravalho, R. G. Tompkins, M. L. Yarmush, and M. Toner. 1994. Effectiveness of poloxamer 188 in arresting calcein leakage from thermally damaged isolated skeletal muscle cells. *In* Electrical Injury: A Multidisciplinary Approach to Therapy, Prevention and Rehabilitation. R. C. Lee, M. Capelli-Schellpfeffer, and K. M. Kelley, editors. *Ann. N. Y. Acad. Sci.* 720:111–123.

Prausnitz, M. R., V. G. Bose, R. Langer, and J. C. Weaver. 1993. Electroporation of mammalian skin: A mechanism to enhance transdermal drug delivery. *Proc. Natl. Acad Sci. U.S.A.* 90:10504–10508.

Quirion, F., and S. St-Pierre. 1991. Reduction of the in vitro hemolytic activity of soybean lecithin liposomes by treatment with a block copolymer. *Biophys. Chem.* 40:129–134.

Rodeheaver, G. T., L. Kurtz, B. J. Kircher, and R. F. Edlich. 1980. Pluronic F-68: a promising new skin wound cleanser. *Ann. Emerg. Med.* 9:572–576.

Sale, A. J. H., and W. A. Hamilton. 1967. Effects of high electric fields on microorganisms. I. Killing of bacteria and yeasts. *Biochim. Biophys. Acta.* 148:781–788.

Schmolka, I. R. 1972. Artificial skin I. Preparation and properties of Pluronic F-127 gels for treatment of burns. *J. Biomed. Mater. Res.* 6:571–582.

Schmolka, I. R. 1975. Artificial blood emulsifiers. *Fed. Proc.* 34: 1449–1453.

Schmolka, I. R. 1977. A review of block polymer surfactants. *J Am. Oil Chem. Soc.* 54:110–116.

Schmolka, I. R. 1994. Physical basis for poloxamer interactions. *In* Electrical Injury: A Multidisciplinary Approach to Therapy, Prevention and Rehabilitation. R. C. Lee, M. Capelli-Schellpfeffer, and K. M. Kelly, editors. *Ann. N. Y. Acad. Sci.* 720:92–97.

Sharma, V., J. C. Murphy, K. Stebe, and L. Tung. 1994a. Poloxamer-188 can reduce conductance and increase stability of artificial bilipid membranes during electroporation. *In* Charge and Field Effects in Biosystems-4, M. J. Allen, S. F. Cleary, and A. E. Sowers, editors. A. E. World Scientific, Singapore. 398–402.

Sharma, V., J. C. Murphy, and L. Tung. 1994b. Interrelationship among breakdown voltage, latency time and membrane conductance during electroporation of artificial lipid membranes. *Proc. Ann. Int. Conf. IEEE Eng. Med. Biol. Soc.* 16:1177–1178.

Sharma, V., and L. Tung. 1995. Poloxamer 188 may decrease the susceptibility of lipid membranes to electroporation. *Trans. 15th Soc. Phys. Reg. Biol. Med.* Washington, D.C. 35.

Sixou, S., and J. Teissie. 1993. Exogenous uptake and release of molecules by electroloaded cells: a digitized videomicroscopy study. *Bioelectrochem. Bioenerg.* 31:237–257.

Sundaram, S., and K. J. Stebe. 1996. Equations for the equilibrium surface pressure increase on the penetration of an insoluble monolayer by a soluble surfactant. *Langmuir.* 12:2028–2034.

Trump, B. F., and I. K. Berezesky. 1995. Calcium-mediated cell injury and cell death. *FASEB J.* 9:219–228.

Tsong, T. Y. 1991. Electroporation of cell membranes. *Biophys. J.* 60: 297–306.

Tung, L. 1992. Electrical injury to heart muscle cells. *In* Electrical Trauma: the Pathophysiology, Manifestation and Clinical Management. R. C. Lee, E. G. Cravalho, and J. F. Burke, editors. Univ. of Cambridge Press, Cambridge, UK.

Tung, L., O. Tovar, M. Neunlist, S. K. Jain, and R. J. O'Neill. 1994. Effects of strong electrical shock on cardiac muscle tissue. *In* Electrical Injury: A Multidisciplinary Approach to Therapy, Prevention and Rehabilitation. R. C. Lee, M. Capelli-Schellpfeffer, and K. M. Kelley, editors. *Ann. N. Y. Acad. Sci.* 720:160–175.

Vanbever, R., N. Lecouturier, and V. Preat. 1994. Transdermal delivery of metoprolol by electroporation. *Pharmacol. Res. Commun.* 11: 1657–1662.

Weaver, J. C. 1995. Electroporation theory. Concepts and mechanisms. *Methods Mol. Cell Biol.* 47:1–26.

Weaver, J. C., and A. Barnett. 1992. Progress toward a theoretical model for electroporation mechanism: membrane electrical behavior and molecular transport. *In* Guide to Electroporation and Electrofusion. D. C. Chang, B. M. Chassy, J. A. Saunders, and A. E. Sowers, editors. Academic Press, New York.

Weingarten, C., N. S. S. Magalhaes, A. Baszkin, S. Benita, and M. Seiller. 1991. Interaction of a non-ionic ABA copolymer surfactant with phospholipid monolayers: possible relevance to emulsion stabilization. *Int. J. Pharmacol.* 75:171–179.

White, S. H. 1972. Analysis of the torus surrounding planar lipid bilayer membranes. *Biophys. J.* 12:432–445.

White, S. H. 1986. The physical nature of planar bilayer membranes. *In* Ion Channels Reconstitution. C. Miller, editor. Plenum Press, New York. 3–32.

White, S. H., and T. E. Thompson. 1973. Capacitance, area, and thickness variations in thin lipid films. *Biochim. Biopys. Acta.* 323:7–22.

Wilhelm, C., M. Winterhalter, U. Zimmermann, and R. Benz. 1993. Kinetics of pore size during irreversible electrical breakdown of lipid bilayer membranes. *Biophys. J.* 64:121–128.

Wolf, H., M. P. Rols, E. Boldt, E. Neumann, and J. Teissie. 1994. Control by pulse parameters of electric field-mediated gene transfer in mammalian cells. *Biophys. J.* 66:524–531.

Zar, J. H. 1984. Biostatistical Analysis. Prentice-Hall Int. Inc., Englewood Cliffs, New Jersey.